

Axisymmetric Magnetic Fields, Electron Capture and Pycnonuclear Reactions in Magnetized White Dwarfs

Edson Otoniel^{1,3,*}, Bruno Franzon^{2,†}, Manuel Malheiro^{1,‡}, Stefan Schramm^{2,§} and Fridolin Weber^{3,¶}

¹*Departamento de Física, Instituto Tecnológico de Aeronáutica, Praça Marechal Eduardo Gomes, 50 - Vila das Acácias, 12228-900 São José dos Campos, SP, Brazil*

²*Frankfurt Institute for Advanced Studies, Ruth-Moufang-1 60438 Frankfurt am Main, Germany and*

³*Department of Physics, San Diego State University,*

5500 Campanile Drive, San Diego, California 92182, USA and

Center for Astrophysics and Space Sciences, University of California at San Diego, La Jolla, California 92093, USA

(Dated: September 21, 2016)

In this work, we study the properties of magnetized white dwarfs taking into account possible instabilities due to electron capture and pycnonuclear fusion reactions in the cores of such objects. The structure of white dwarfs is obtained by solving the Einstein-Maxwell equations with a poloidal magnetic field in a fully general relativistic approach. The stellar interior is composed of a regular crystal lattice made of carbon ions immersed in a degenerate relativistic electron gas. The onsets of electron capture reactions and pycnonuclear reactions are determined with and without magnetic fields. We find that magnetized white dwarfs violate the standard Chandrasekhar mass limit significantly, even when electron capture and pycnonuclear instabilities are present in the stellar interior. We obtain a maximum white dwarf mass of around $2.12 M_{\odot}$ with a central magnetic field of $\sim 1.74 \times 10^{14}$ G, which indicates that magnetized white dwarfs may be the progenitor candidates of superluminous type Ia supernovae. Furthermore, we show that the critical density for pycnonuclear fusion reactions limits the central white dwarf density up to 2.39×10^9 g/cm³ and, as a consequence, its equatorial radius cannot be smaller than $R \sim 1600$ km. Finally, we find for magnetized white dwarfs with central magnetic field lower than $\sim 10^{13}$ G the usual phenomenology known in the literature: increasing the central magnetic field (the magnetic energy density), the central baryonic number density reduces and the stellar radius increases. However, for higher central magnetic fields (and higher masses), we have a new phenomenology for the star structure: increasing the magnetic field of the star, the central baryonic number density increases proportionally, since the equatorial radius decreases, making ultramagnetized white dwarfs more compact.

I. INTRODUCTION

It is generally accepted that stars born with masses below around 10 solar masses end up their evolutions as white dwarfs (WDs) [1–3]. With a typical composition mostly made of carbon, oxygen, or helium, white dwarfs possess central densities up to $\sim 10^{11}$ g/cm³. They can be very hot [4], fast rotating [5–7] and strongly magnetized [8, 9]. The observed surface magnetic fields range from 10^6 G to 10^9 G [10–15]. The internal magnetic fields of white dwarfs are not known, but they are expected to be larger than their surface magnetic fields. This is due to the fact that in ideal magneto hydrodynamics (MHD), the magnetic field, B , is ‘frozen’ with the fluid and $B \propto \rho$, with ρ being the local mass density (see, e.g., Refs. [16, 17]). A simple estimate follows from the virial theory by equating the magnetic field energy with the gravitational binding energy, which leads to an upper limit for the magnetic fields inside of WDs of $\sim 10^{13}$ G. On the other hand, analytic and numeric calculations, both in Newtonian theory as well as in General Relativity

theory, show that WDs may have internal magnetic fields as large as 10^{12-16} G (see, e.g., Refs. [2, 15, 18–20]).

The relationship between the gravitational stellar mass, M , and the radius, R , of non-magnetized white dwarfs was first determined by Chandrasekhar [21]. Recently, mass-radius relationships of magnetic white dwarfs have been discussed in the literature (see, e.g., Refs. [18, 20, 22]). These studies show that the masses of white dwarfs increases in the presence of strong magnetic fields. This is due to the Lorentz force, which acts against gravity and, therefore, supporting more massive white dwarfs.

Based on recent observations of several superluminous type Ia supernovae [23–29], it has been suggested that the progenitor mass of such explosions (SN 2006gz, SN 2007if, SN 2009dc, SN 2003fg) significantly exceeds the Chandrasekhar mass limit of $M_{\text{Ch}} \sim 1.4 M_{\odot}$ [30]. Super-heavy progenitors were studied as a result of mergers of two massive white dwarfs [31–33]. Alternatively, the authors of Ref. [34] obtained super-Chandrasekhar white dwarfs for magnetically charged stars. In addition, super-Chandrasekhar white dwarfs were investigated in the presence of strong magnetic fields in Refs. [35]. In Refs. [36, 37], WDs models with magnetic fields were calculated in the Newtonian framework. A recent study of differentially rotating, magnetized white dwarfs has shown that differential rotation might increase the mass of magnetized white dwarfs up to $3.1 M_{\odot}$ [38]. According

* edson.otoni@gmail.com

† franzon@fias.unifrankfurt.de

‡ malheiro@ita.br

§ schramm@fias.unifrankfurt.de

¶ fweber@mail.sdsu.edu

to Ref. [39], purely toroidal magnetic field components can raise white dwarfs masses up to $5 M_\odot$.

According to Refs. [40], effects of an extremely large and uniform magnetic field on the equation of state (EOS) of a white dwarf would increase its critical mass up to $2.58 M_\odot$. This mass limit is reached for extremely large magnetic fields of $\sim 10^{18}$ G. Nevertheless, as already shown in Refs. [41, 42], the breaking of spherical symmetry due to magnetic fields and micro-physical effects, such as electron capture reactions and pycnonuclear reactions, can severely limit the magnetic field inside white dwarfs.

In Ref. [20], we obtained mass-radius relationships of highly magnetized white dwarfs, using a pure degenerate electron Fermi gas to describe the massive matter inside WDs. However, according to Ref. [43], many-body corrections modify the EOS and, therefore, the mass-radius relationship of white dwarfs. Hence, in this paper, we use an EOS which takes into account not only the electron Fermi gas contribution, but also electron-ion interactions (regular lattice) as recently calculated in Ref. [44], taking into account microscopic stability issues related to electron capture and pycnonuclear reactions in the cores of WDs.

This paper is structured as follows. In Sec. II we discuss the input physics, i.e., the equation of state and composition of white dwarf matter. In Sec. III, we briefly discuss the equations that are being solved numerically to obtain the structure of stationary magnetized white dwarfs. In Sec. IV, we discuss our findings. We conclude our paper with a summary, which is provided in Sec. V.

II. STELLAR INTERIOR

The properties of fermionic matter were studied many decades ago in Refs. [43, 45]. Typically, a white dwarf is composed of atomic nuclei immersed in a fully ionized electron gas. In this work, in addition to electron-ion interactions for an ionic lattice structure, we make use of the latest experimental atomic mass data [46, 47] to obtain the equation of state. The model adopted here to describe the nuclear lattice was derived for the outer crust of neutron stars in Refs. [42, 48] and later applied to WDs in Ref. [49]. According to this model, the core of white dwarfs are subjected to the degenerate electron and ionic lattice pressures. The total pressure is then given by:

$$P = P_e + P_L(Z, Z'), \quad (1)$$

where P_e denotes the electron pressure determined in [43] and $P_L(Z, Z')$ the lattice pressure for two different type of ions. The lattice pressure is given by the energy density of the ionic lattice (see Ref. [48]):

$$P_L(Z, Z') = \frac{1}{3} \mathcal{E}_L, \quad (2)$$

with Z and Z' being the proton number of two different ions. In our case, the white dwarf is composed of carbon ions, i.e., $Z'=Z=12$. However, for the sake of completeness, we keep the dependence of Z' in the equations. Following the Bohrvan Leeuwen theorem [48], the lattice energy density arranged in a regular crystal structure (single cubic) does not depend on the magnetic field. In this case, the lattice energy density reads [42]:

$$\mathcal{E}_L = C e^2 n_e^{4/3} G(Z, Z'), \quad (3)$$

with $G(Z, Z')$ given by:

$$G(Z, Z') = \frac{\alpha Z^2 + \gamma Z'^2 + (1 - \alpha - \gamma) Z Z'}{(\xi Z + (1 - \xi) Z')^{4/3}}. \quad (4)$$

The quantities C , α , γ are lattice constants and ξ is the ratio of ions A_ZY and ${}^{A'}_{Z'}Y$ in the lattice [49] (see Table I). If only a single ion is present in the lattice, Eq. 4 does not depend on α and γ , and Eq. 3 becomes:

$$\mathcal{E}_L = C e^2 n_e^{4/3} Z^{2/3}, \quad (5)$$

The energy density is given by an appropriate combination of the degenerate electron energy, the energy density of the ions, and the energy density of the ionic lattice,

$$\mathcal{E} = n_x M(Z, A) c^2 + n_{x'} M(Z', A') c^2 + \mathcal{E}_e + \mathcal{E}_L - n_e m_e c^2, \quad (6)$$

where n_x and $n_{x'}$ are the number densities of the respective atomic nuclei, and $M(Z, A)$ and $M(Z', A')$ stand for the most recent experimental nuclear masses (see Refs. [46, 47]).

	C	α	γ	$(1 - \alpha - \gamma)$	ξ
sc	-1.418649	0.403981	0.403981	0.192038	0.5

TABLE I. Lattice constants C , α , γ and parameters $(1 - \alpha - \gamma)$ and ξ for a simple cubic structure (sc), as obtained by the method of Coldwell-Horsfall and Maradudin (see Chamel *et al.* [49]).

A. Instabilities in strongly magnetized white dwarfs

As shown in Refs. [49, 50], white dwarfs can be unstable due to inverse β -decay. A schematic illustration of this reaction is given by $A(N, Z) + e^- \rightarrow A(N + 1, Z - 1) + \nu_e$. Because of this reaction, atomic nuclei become more neutron rich and the energy density of the matter is being reduced, at a given pressure, leading to a softer EOS. In addition to the inverse β -decay, pycnonuclear reactions are believed to occur in the cores of white dwarfs too (see Refs. [46, 47]). These nuclear fusion reactions occur among heavy neutron-rich atomic nuclei [49].

The rates of these types of reactions, however, are still uncertain. Electron capture and pycnonuclear reaction processes can be estimated as [42]:

$$\rho_\beta > \rho_\beta^{\min} = \frac{B^\beta(A, Z)^{3/2}}{\sqrt{2}\pi^2\lambda^3} \frac{A}{Z} m, \quad (7)$$

and

$$\rho_{\text{pyc}} > \rho_{\text{pyc}}^{\min} = \frac{B^\beta(2A, 2Z)^{3/2}}{\sqrt{2}\pi^2\lambda^3} \frac{A}{Z} m, \quad (8)$$

where m is the neutron mass, λ is the electron Compton wavelength and

$$B^\beta(A, Z) \equiv \frac{1}{2} \left(\frac{\mu_e^\beta(A, Z)}{m_e c^2} \right)^2.$$

For the electron chemical potential one has [46, 47]:

$$\mu_e \geq \mu_e^\beta(A, Z) \equiv \Delta(A, Z - 1) - \Delta(A, Z) + m_e c^2$$

where $\Delta(A, Z)$ denotes the excess mass of the nuclei, which, for magnetic field strengths $< 10^{17}$ G, is independent of the magnetic field [42].

The values of the density thresholds of the inverse β -decay and pycnonuclear reactions for magnetic white dwarfs with $B = 10^{12-15}$ G composed of carbon are given in the Table II.

$\rho_\beta^{B=0}$	$\rho_\beta^{B=10^{12-15}}$	$\rho_{\text{pyc}}^{B=0}$	$\rho_{\text{pyc}}^{B=10^{12-15}}$
$^{12}\text{C } 3.94 \times 10^{10}$	2.93×10^{10}	3.22×10^9	2.39×10^9

TABLE II. Value of Inverse β -reaction and pycnonuclear reaction to magnetized ($B = 10^{12-15}$ G) and non-magnetized electron gas constituted by carbon in the unit g/cm^3

In Fig. 1, we show white dwarf equations of state with and without lattice contributions. The black lines (no lattice contribution) and red dashed line (with lattice contribution) are for white dwarf matter with zero magnetic field ($B = 0$). The vertical lines show the density thresholds of the inverse β -decay and pycnonuclear reactions (see Table II). The softening of the EOS due to lattice contributions is shown in the illustration on the right-hand-side of Fig. 1.

III. WHITE DWARFS WITH AXISYMMETRIC MAGNETIC FIELDS

The numerical technique used in this work to study axisymmetric magnetic fields was first applied to neutron stars in Refs. [51, 52], and more recently in Ref. [53–55]. The same formalism was used to study rotating and magnetized white dwarfs in Ref. [20]. Here we build stellar equilibrium configurations by solving the Einstein-Maxwell field equations in a fully general relativistic approach. For more details about the theoretical formalism and numerical procedure, see e.g., Ref. [56]. Below

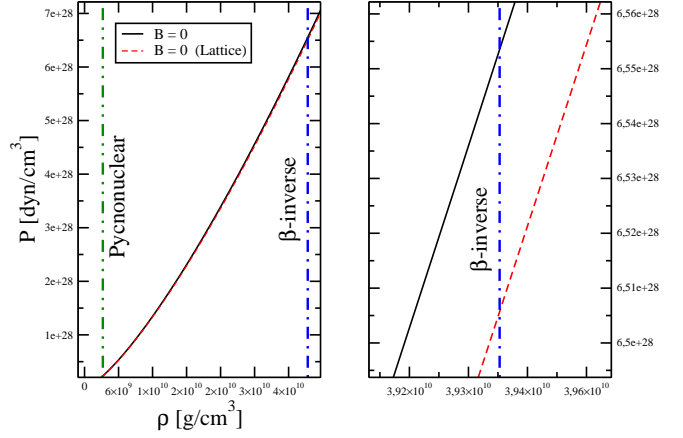


FIG. 1. (Color online) Equation of state for $B = 0$ with (dashed red curve) and without (solid black curves) lattice contributions. The high-density portion of the figure on the left is magnified in the figure on the right-hand-side.

we show the basic electromagnetic equations which, combined with the gravitational equations, are solved numerically by means of a spectral method. In this context, the stress-energy tensor $T_{\alpha\beta}$ is composed of the matter and the electromagnetic source terms:

$$T_{\alpha\beta} = (e+p)u_\alpha u_\beta + p g_{\alpha\beta} + \frac{1}{\mu_0} \left(F_{\alpha\mu} F_{\beta}^\mu - \frac{1}{4} F_{\mu\nu} F^{\mu\nu} g_{\alpha\beta} \right), \quad (9)$$

with $F_{\alpha\mu}$ being the antisymmetric Faraday tensor defined as $F_{\alpha\mu} = \partial_\alpha A_\mu - \partial_\mu A_\alpha$, where A_μ is the non-zero components of the electromagnetic four-potential, $A_\mu = (A_t, 0, 0, A_\phi)$. The total energy density of the system is e , the pressure is denoted by p , u_α is the fluid 4-velocity, and the metric tensor is $g_{\alpha\beta}$. The first term in Eq. (9) represents the isotropic matter contribution to the energy momentum-tensor, while the second term is the anisotropic electromagnetic field contribution.

The metric tensor in this axisymmetric spherical-like coordinates (r, θ, ϕ) can be expressed as:

$$ds^2 = -N^2 dt^2 + \Psi^2 r^2 \sin^2 \theta (d\phi - N^\phi dt)^2 + \lambda^2 (dr^2 + r^2 d\theta^2), \quad (10)$$

with N , N^ϕ , Ψ and λ being functions of the coordinates (r, θ) , see Ref. [51] for more details. As in Ref. [51], the equation of motion for a star endowed with magnetic fields reads:

$$H(r, \theta) + \nu(r, \theta) + M(r, \theta) = \text{const}, \quad (11)$$

where $H(r, \theta)$ is the heat function defined in terms of the baryon number density n ,

$$H = \int_0^n \frac{1}{e(n_1) + p(n_1)} \frac{dP}{dn}(n_1) dn_1. \quad (12)$$

The quantity $\nu(r, \theta)$ in Eq. (11) is defined as $\nu = \ln N$,

and the magnetic potential $M(r, \theta)$ is given by:

$$M(r, \theta) = M(A_\phi(r, \theta)) \equiv - \int_{A_\phi(r, \theta)}^0 f(x) dx, \quad (13)$$

with $f(x)$ being the current function. The magnetic stellar models are obtained by assuming a constant value f_0 for the dimensionless current functions [54]. According to Ref. [52], other choices for $f(x)$ are possible, but the general conclusions remain the same.

IV. RESULTS

In this section, we discuss the effects of strong magnetic fields on the global properties of stationary white dwarfs taking into account instabilities due to inverse β -decay and pycnonuclear reactions. In addition, we make use of an equation of state for the matter that includes both the electron-ion interactions and the latest experimental atomic mass data. The instabilities related to the microphysics are fundamental since they restrict equilibrium configurations and constrain the maximum magnetic fields that these stars can have [42]. In addition to magnetic profiles obtained by assuming constant current functions, f_0 , as already done in Ref. [20], we solve the stellar models at constant magnetic dipole moments μ . In Ref. [20], a simple Fermi gas was used and the microphysical issues were not addressed. In this work, the maximum white dwarf mass for non-magnetized stars is smaller than the one considered in Ref. [20], since the lattice contribution softens the EOS.

In Fig. 2, we show the relation between the gravitational mass and central density for a sequence of stars at different fixed magnetic dipole moments μ and current function f_0 . The magnetic dipole moment μ is defined as (see Ref. [51])

$$\frac{2\mu \cos \theta}{r^3} = B(r) |_{r \rightarrow \infty}, \quad (14)$$

which is simply the radial component (the orthonormal one) of the magnetic field of a magnetic dipole seen by an observer at infinity. As can be seen from Fig. 2, a larger magnetic moment μ leads first to an increase in the white dwarf maximum mass. However, if we increase μ further, the maximum mass drops. This is due to the fact that the stellar radius becomes larger (see also Fig. 3) and, therefore, the magnetic field (see Eq. 14) is reduced. As a result, the Lorentz force gets proportionally smaller, making the maximum stellar masses configurations less massive.

In Fig. 2, we show the mass-central density relation of magnetized white dwarfs for a range of different f_0 and μ values. This relation is monotonic for a fixed value of μ , but non-monotonic (in some cases even multivalued) if f_0 is kept fixed. The cyan area in Fig. 2 represents the density regime where pycnonuclear reactions set in and the black square marks the gravitational mass of a

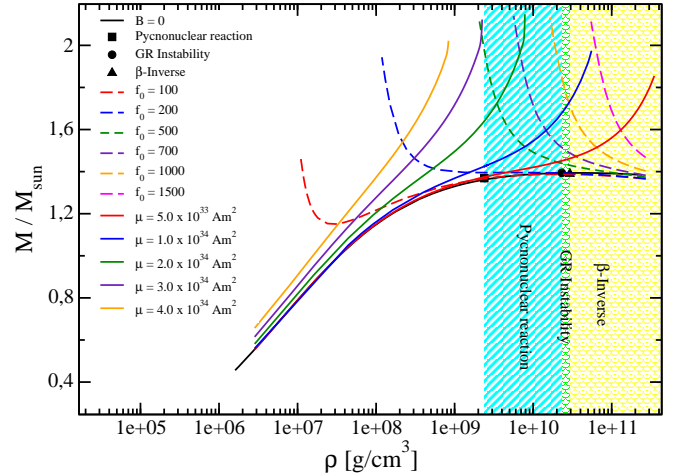


FIG. 2. (Color online) Gravitational mass as a function of central mass density for magnetized white dwarfs assuming different constant current functions, f_0 , and different magnetic dipole moments, μ . The shaded areas represent the onset of pycnonuclear reactions and the density thresholds for inverse β -decay. (see TABLE II)

star without magnetic field at the onset of this region. The green area shows the general relativistic instability (labeled GR Instability), with the black circle marking the gravitational mass of the star associated with that instability. In addition, from Fig. 2, we see that the condition $\frac{dM}{d\rho_c} > 0$ is satisfied along the curves at fixed magnetic dipole moments μ . This is the condition that indicates stability of the spherical and non-magnetized stars against radial oscillations.

According to our calculations, the GR instability happens before the inverse- β decay. It is worth mentioning that we make use of carbon ($A/Z=2$) for the initial internal composition of the white dwarfs. The threshold for inverse β -decay reactions is represented by the yellow area. As can be seen in Fig. 2, the critical density for pycnonuclear fusion reactions limits the central white dwarf density up to $2.39 \times 10^9 \text{ g/cm}^3$, what constrains the equatorial radius in $R \sim 1600 \text{ km}$ (see Fig. 3). The maximum white dwarf mass (end point of the curve $\mu = 3 \times 10^{34} \text{ Am}^2$), which is outside the microscopic instability regions, is $\sim 2.12 M_\odot$ and the equatorial radius of this star is $\sim 1596 \text{ km}$.

According to Eq. (14), the magnetic field of a star is determined by the magnetic dipole moment μ and the stellar radius. In Fig. 3, we show the mass-radius relationship for magnetized white dwarfs for different magnetic dipole moments μ . From Fig. 3, we see that stars become bigger for larger values of μ . The magnetic field strength, however, can not be extracted from Fig. 3. In order to do so, we depict in Fig. 4 the gravitational mass as a function of surface (B_s) and central (B_c) magnetic fields, the circumferential equatorial radius (R_{circ}) and

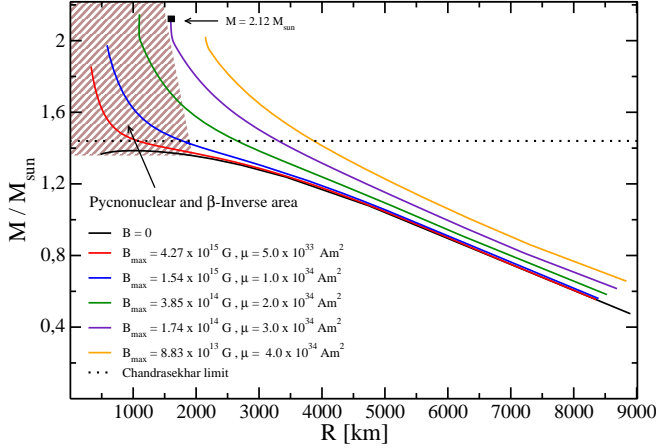


FIG. 3. (Color online) Mass-radius relationship for magnetized white dwarfs assuming different magnetic dipole moments, μ . The black line represents the mass-radius relationship of non-magnetized white dwarfs. The horizontal line represents the Chandrasekhar mass limit for spherical stars. Also shown are the values of the central magnetic field B_{max} (with the corresponding magnetic dipole moment μ) reached at the center of maximum mass stars (end point of the curve with fixed μ). White dwarfs located in the brown region are subject to pycnonuclear or inverse β -decay reactions.

the baryon number density (n_b) for two different magnetic dipole moments $\mu = 0.5 \times 10^{34} \text{ Am}^2$ (red line) and $\mu = 4.0 \times 10^{34} \text{ Am}^2$ (orange line). One can choose other values of μ for this comparison, but the conclusions remain the same.

In Fig. 4, there is a crossing point between the curves with $\mu = 0.5 \times 10^{34} \text{ Am}^2$ and $\mu = 4.0 \times 10^{34} \text{ Am}^2$. This is due to the fact that the magnetic field scales as $\sim \frac{\mu}{r^3}$, with r being the coordinate radius, which is the stellar radius within the domain of the star. Stars with fixed baryon masses of $M_B = 1.00 M_\odot$ and $M_B = 1.80 M_\odot$ are represented by dashed horizontal lines in Fig. 4. According to Eq. (14), along different (but fixed) μ curves, the magnetic field is determined only by the size of the star. However, along the fixed baryon mass lines, the magnetic field is a combination of the magnetic dipole moment μ and the coordinate radius r .

Looking at the relation between the stellar masses and the surface and central magnetic fields in the diagrams $M \times B_s$ and $M \times B_c$ in Fig. 4, one sees that stars (at fixed baryon masses) above the crossing point of the curves $\mu = 0.5 \times 10^{34} \text{ Am}^2$ (red line) and $\mu = 4.0 \times 10^{34} \text{ Am}^2$ (orange line) possess higher magnetic fields for lower magnetic dipole moments. In this case, a stellar sequence, for example with $M_B = 1.80 M_\odot$, from highly magnetized to less magnetized white dwarfs (indicated by black arrows) would be followed by an increase in their magnetic dipole moments, from $\mu = 0.5 \times 10^{34} \text{ Am}^2$ to $\mu = 4.0 \times 10^{34} \text{ Am}^2$. This is accompanied by an increase in the stellar ra-

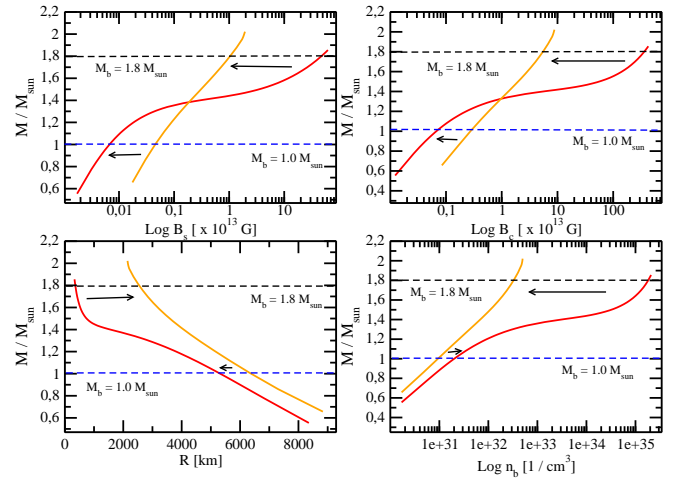


FIG. 4. (Color online) Global properties of magnetized white dwarfs for two different magnetic dipole moments, $\mu = 0.5 \times 10^{34} \text{ Am}^2$ (red line) and $\mu = 4.0 \times 10^{34} \text{ Am}^2$ (orange line). The horizontal lines represent white dwarfs with fixed baryon masses of $M_B = 1.00 M_\odot$ and $M_B = 1.80 M_\odot$, respectively. The arrows indicate a possible magnetic field reduction in these stars (see text for details).

dius (see diagram $M \times R_{circ}$) and a decrease in the central baryon density (see diagram $M \times n_b$). On the other hand, below the crossing point, stars at fixed baryon masses have a reduction in their magnetic fields by decreasing their magnetic dipole moments (black arrows). In this case, white dwarfs become smaller and, therefore, more dense at the center (see $M \times R_{circ}$ and $M \times n_b$ diagrams of Fig. 4 for $M_B = 1.00 M_\odot$).

In Fig. 4, it is interesting that stars with masses above the crossing point expand in the equatorial radius at the same time that their magnetic fields reduce. Note that, as the magnetic dipole moment increases, the star (at fixed baryon masses) expands in the equatorial direction due to the Lorentz force. However, the stellar magnetic field scales as $\frac{\mu}{r^3}$. It means that for a star with $M_B = 1.80 M_\odot$, the increase in the magnetic dipole moment μ is canceled by the increase in the radius, reducing the magnetic field. This is the opposite as expected for stars with lower masses. For example, a star with $M_B = 1.00 M_\odot$ decreases its magnetic dipole moment and its radius. However, in this case, the decrease in the radius is not enough to cancel the decrease in μ . As a result, the magnetic field decreases proportionally. This can be understood by looking at the variation in the circular equatorial radius for the stars $M_B = 1.80 M_\odot$ and $M_B = 1.00 M_\odot$. In the last case, one has ΔR_{circ} much smaller than ΔR_{circ} for $M_B = 1.80 M_\odot$ for the same (absolute) variation in the magnetic dipole moment, namely, $|\Delta \mu| = 3.5 \times 10^{34} \text{ Am}^2$.

In Fig. 5, we show the global properties of two white dwarfs at fixed baryon masses of $M_B = 1.00 M_\odot$ and $M_B = 1.80 M_\odot$, respectively. In the top panel we depict the central baryon density as a function of the central

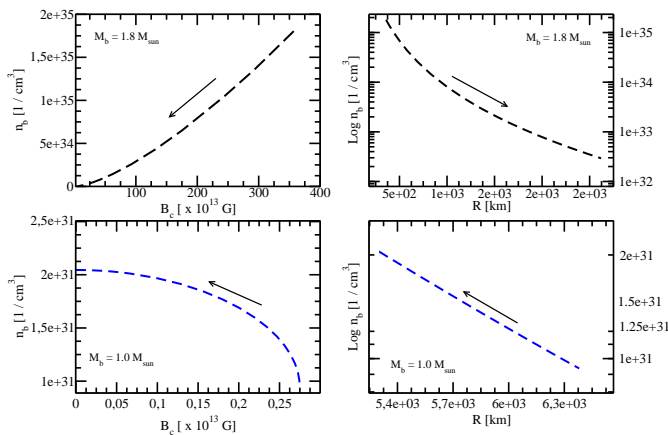


FIG. 5. Central baryon number density as a function of magnetic field strength and circular equatorial radius for magnetized white dwarfs with fixed baryon masses of $M_B = 1.00 M_\odot$ and $M_B = 1.80 M_\odot$.

magnetic field and the circular equatorial radius for a star with $M_B = 1.80 M_\odot$. In this case, as the magnetic field decreases, the central baryon density becomes smaller, due to the fact that the radius is increasing. On the other hand, a star with $M_B = 1.00 M_\odot$ increases its central baryon density as the magnetic field decreases, since the stellar radius is reduced.

V. SUMMARY

In this paper, we present axisymmetric and stationary models of magnetized white dwarfs obtained by solving the Einstein-Maxwell equations self-consistently taking into consideration stability issues related to neutronization due to electron capture and pycnonuclear reactions between carbon nuclei inside such objects.

As discussed by many authors [18–20, 40, 57], magnetized white dwarfs can be progenitors of some peculiar superluminous type Ia supernovae (e.g., SN 2006gz, SN 2007if, SN 2009dc, SN 2003fg). A possible mechanism for the formation of magnetized white dwarfs was proposed in Ref. [57]. According to these studies, the stars are formed by accretion onto a commonly observed magnetized white dwarf. A type Ia supernova event would be triggered when a spherical and non-magnetized white dwarf approaches its maximum (Chandrasekhar) mass. The Lorentz force induced by strong magnetic fields breaks the spherical symmetry of stars and increases the mass of the star, since the force acts in the radial outward direction against the inwardly directed gravitational pull.

We make use of an equation of state for a degenerate electron gas with electron-ion interactions (simple cubic) to describe the matter inside of white dwarfs. We have shown that the equation of state becomes softer if nuclear lattice contributions are included in addition to the electron pressure. This is due to the fact that the re-

pulsive force between electrons is smaller in the presence of an ionic lattice, causing a softening of the equation of state (see Fig. 1). We note that the density thresholds for pycnonuclear and inverse β -reactions are reduced when magnetic fields are present in the stellar interior, as can be seen in Table II.

We have shown that the masses of white dwarfs increase up to $M = 2.12 M_\odot$ (with a corresponding magnetic dipole moment of $\mu = 3.0 \times 10^{34} Am^2$ (see, e.g., Fig. 2) if microphysical instabilities are considered. This star has an equatorial radius of ~ 1596 km with magnetic fields of $B_c = 1.74 \times 10^{14} G$ and $B_s = 3.6 \times 10^{13} G$ at the center and at the stellar surface, respectively. For this white dwarf, the ratio between the matter pressure and the magnetic pressures is 0.867. In this work, the maximum magnetic field found is an order of magnitude smaller than in Ref. [20]. This is because we modeled the stellar interior with a much more realistic equation of state than just a simple electron gas, and we considered the density threshold for pycnonuclear fusion reactions, which restricts the central density of white dwarfs in $\sim 2.39 \times 10^9$ g/cm³ (see Table II), limiting the stellar masses and, therefore, their radii, which for very massive and magnetized white dwarfs cannot be smaller than $R \sim 1600$ km.

Our results show that the surface magnetic field, B_s , is about one order of magnitude smaller than the magnetic field reached at the stellar center, B_c . Assuming that the magnetic field decays over time, we have seen that massive white dwarfs (at fixed baryon mass) reduce their magnetic fields while their magnetic dipole moments increase. This is due to the fact that at fixed baryon mass, the magnetic field is determined by the interplay between the magnetic dipole moment and the stellar radius. For less massive white dwarfs, we found that the smaller the magnetic field, the smaller the magnetic dipole moment. However, we found that some massive and magnetized white dwarfs decrease their magnetic fields, by expanding the equatorial radius, even when their magnetic dipole moments increase. Thus, we found a new phenomenology for very massive white dwarfs with central magnetic fields higher than $B \sim 10^{13}$ G, i.e., increasing the magnetic field, the central baryonic number density increases as well, since the equatorial radius decreases. This phenomenology differs from previous calculations for magnetic fields lower than $\sim 10^{13}$ G [22, 37], where the increase in the central magnetic field (the magnetic energy density) makes the star less dense and larger.

We note that stellar configurations which contain only poloidal magnetic fields (no toroidal component) are unstable (see, e.g., [58–60]). Recently, a perturbation study of axisymmetric, strongly magnetic degenerate stars was performed in Ref. [61], where the instability appears after about an Alfvén crossing time. Moreover, according to Ref. [62], many different mechanisms can affect the magnetic field strengths and its distributions inside of the stars. In this work, in the framework of a fully general relativistic treatment, we model the properties of

magnetized white dwarfs with purely poloidal magnetic field components. Although this is not the most general magnetic field profile, such stars can considerably increase their masses due to magnetic field effects, even when microphysical instabilities are considered. As a result, such white dwarfs can be possible candidates of the super-Chandrasekhar mass white dwarfs and, thereby, contribute to superluminous type-Ia supernovae.

The Landau energy levels of electrons are modified by relativistic effects for magnetic fields higher than the QED magnetic field strength of $B_{cr} = 4.4 \times 10^{13} G$. In the future, we are going to take into account magnetic field configurations with both poloidal and toroidal components, as well magnetic field corrections in the equation of state. We expect that the findings presented in this paper are not going to change qualitatively, since

the leading contribution to the macroscopic properties of stars, like gravitational mass and radius, ought to come from the pure field contribution of the energy-momentum tensor. Work along this line is in progress.

VI. ACKNOWLEDGMENTS

We acknowledge financial support from the Brazilian agencies CAPES, CNPq, and we would like to thank FAPESP for financial support under the thematic project 13/26258-4 B. Franzon acknowledges support from CNPq/Brazil, DAAD and HGS-HIRE for FAIR. S. Schramm acknowledges support from the HIC for FAIR LOEWE program. F. Weber is supported by the National Science Foundation (USA) under Grant PHY-1411708.

-
- [1] F. Weber, *Pulsars as astrophysical laboratories for nuclear and particle physics* (CRC Press, 1999).
 - [2] S. L. Shapiro and S. A. Teukolsky, *Black holes, white dwarfs and neutron stars: the physics of compact objects* (2008).
 - [3] N. K. Glendenning, *Compact stars: Nuclear physics, particle physics and general relativity* (Springer Science & Business Media, 2012).
 - [4] L. G. Althaus, J. A. Panei, M. M. M. Bertolami, E. Garca-Berro, A. H. Corsico, A. D. Romero, S. Kepler, and R. D. Rohrmann, *The Astrophysical Journal* **704**, 1605 (2009).
 - [5] G. Arutyunyan, D. Sedrakyan, and É. Chubaryan, *Soviet Astronomy* **15**, 390 (1971).
 - [6] K. Boshkayev, J. A. Rueda, R. Ruffini, and I. Siutsou, *The Astrophysical Journal* **762**, 117 (2013).
 - [7] J. B. Hartle, *The Astrophysical Journal* **150**, 1005 (1967).
 - [8] J. G. Coelho, R. M. Marinho, M. Malheiro, R. Negreiros, D. L. Cáceres, J. A. Rueda, and R. Ruffini, *Astrophys. J.* **794**, 86 (2014), arXiv:1306.4658 [astro-ph.SR].
 - [9] R. V. Lobato, M. Malheiro, and J. G. Coelho, *International Journal of Modern Physics D* **25**, 1641025 (2016), <http://www.worldscientific.com/doi/pdf/10.1142/S021827181641025X>.
 - [10] Y. Terada, T. Hayashi, M. Ishida, K. Mukai, T. u. Dotani, S. Okada, R. Nakamura, S. Naik, A. Bamba, and K. Makishima, *Publ. Astron. Soc. Jap.* **60**, 387 (2008), arXiv:0711.2716 [astro-ph].
 - [11] D. Reimers, S. Jordan, D. Koester, N. Bade, T. Kohler, and L. Wisotzki, *Astron. Astrophys.* **311**, 572 (1996), arXiv:astro-ph/9604104 [astro-ph].
 - [12] G. D. Schmidt and P. S. Smith, *Astrophys. J.* **448**, 305 (1995).
 - [13] J. C. Kemp, J. B. Swedlund, J. D. Landstreet, and J. R. P. Angel, *Astrophys. J.* **161**, L77 (1970).
 - [14] A. Putney, *The Astrophysical Journal Letters* **451**, L67 (1995).
 - [15] J. Angel, *Annual Review of Astronomy and Astrophysics* **16**, 487 (1978).
 - [16] L. Mestel, *Stellar magnetism*, Vol. 154 (OUP Oxford, 2012).
 - [17] L. D. Landau, E. M. Lifshitz, J. B. Sykes, J. S. Bell, and M. E. Rose, *Physics Today* **11**, 56 (1958).
 - [18] P. Bera and D. Bhattacharya, *Monthly Notices of the Royal Astronomical Society* **445**, 3951 (2014).
 - [19] P. Bera and D. Bhattacharya, *Monthly Notices of the Royal Astronomical Society* **456**, 3375 (2016).
 - [20] B. Franzon and S. Schramm, *Phys. Rev.* **D92**, 083006 (2015), arXiv:1507.05557 [astro-ph.SR].
 - [21] S. Chandrasekhar, *An Introduction to the Study of Stellar Structure* (Chicago : Univ. Chicago Press, 1939).
 - [22] I.-S. Suh and G. Mathews, *The Astrophysical Journal* **530**, 949 (2000).
 - [23] J. M. Silverman, M. Ganeshalingam, W. Li, A. V. Filippenko, A. A. Miller, and D. Poznanski, *Monthly Notices of the Royal Astronomical Society* **410**, 585 (2011).
 - [24] R. A. Scalzo *et al.*, *Astrophys. J.* **713**, 1073 (2010), arXiv:1003.2217 [astro-ph.CO].
 - [25] D. A. Howell *et al.* (SNLS), *Nature* **443**, 308 (2006), arXiv:astro-ph/0609616 [astro-ph].
 - [26] M. Hicken, P. M. Garnavich, J. L. Prieto, S. J. Blondin, D. L. DePoy, R. P. Kirshner, and J. Parrent, *Astrophys. J.* **669**, L17 (2007), arXiv:0709.1501 [astro-ph].
 - [27] M. Yamanaka *et al.*, *Astrophys. J.* **707**, L118 (2009), arXiv:0908.2059 [astro-ph.HE].
 - [28] S. Taubenberger, S. Benetti, M. Childress, R. Pakmor, S. Hachinger, P. Mazzali, V. Stanishev, N. Elias-Rosa, I. Agnoletto, F. Bufano, *et al.*, *Monthly Notices of the Royal Astronomical Society* **412**, 2735 (2011).
 - [29] S. O. Kepler, S. J. Kleinman, A. Nitta, D. Koester, B. G. Castanheira, O. Giovannini, A. F. M. Costa, and L. Althaus, *Monthly Notices of the Royal Astronomical Society* **375**, 1315 (2007), <http://mnras.oxfordjournals.org/content/375/4/1315.full.pdf+html>.
 - [30] M. Ilkov and N. Soker, *Monthly Notices of the Royal Astronomical Society* **419**, 1695 (2012), <http://mnras.oxfordjournals.org/content/419/2/1695.full.pdf+html>.

- [31] R. Moll, C. Raskin, D. Kasen, and S. Woosley, *Astrophys. J.* **785**, 105 (2014), arXiv:1311.5008 [astro-ph.HE].
- [32] S. Ji, R. T. Fisher, E. Garca-Berro, P. Tzeferacos, G. Jordan, D. Lee, P. Lorn-Aguilar, P. Cremer, and J. Behrends, *The Astrophysical Journal* **773**, 136 (2013).
- [33] D. R. van Rossum, R. Kashyap, R. Fisher, R. T. Wollaeger, E. Garca-Berro, G. Aznar-Sigun, S. Ji, and P. Lorn-Aguilar, *The Astrophysical Journal* **827**, 128 (2016).
- [34] H. Liu, X. Zhang, and D. Wen, *Physical Review D* **89**, 104043 (2014).
- [35] U. Das and B. Mukhopadhyay, *Modern Physics Letters A* **29**, 1450035 (2014).
- [36] D. Adam, *Astronomy and Astrophysics* **160**, 95 (1986).
- [37] J. P. Ostriker and F. Hartwick, *The Astrophysical Journal* **153**, 797 (1968).
- [38] S. Subramanian and B. Mukhopadhyay, *Monthly Notices of the Royal Astronomical Society* **454**, 752 (2015), <http://mnras.oxfordjournals.org/content/454/1/752.full.pdf> + [56].
- [39] P. Bera and D. Bhattacharya, *Monthly Notices of the Royal Astronomical Society* **456**, 3375 (2016), arXiv:1608.02845 [astro-ph.HE].
- [40] U. Das and B. Mukhopadhyay, *Physical Review D* **86** (2012), 10.1103/PhysRevD.86.042001.
- [41] J. G. Coelho, R. M. Marinho, M. Malheiro, R. Negreiros, D. L. Cceres, J. A. Rueda, and R. Ruffini, *The Astrophysical Journal* **794**, 86 (2014).
- [42] N. Chamel, A. F. Fantina, and P. J. Davis, *Physical Review D* **88** (2013), 10.1103/PhysRevD.88.081301.
- [43] E. E. Salpeter, *The Astrophysical Journal* **134**, 669 (1961).
- [44] N. Chamel and A. F. Fantina, *Phys. Rev. D* **92**, 023008 (2015).
- [45] T. Hamada and E. E. Salpeter, *The Astrophysical Journal* **134**, 683 (1961).
- [46] M. Wang, G. Audi, A. H. Wapstra, F. G. Kondev, M. MacCormick, X. Xu, and B. Pfeiffer, *Chinese Physics C* **36**, 1603 (2012).
- [47] G. Audi, M. Wang, A. H. Wapstra, F. G. Kondev, M. MacCormick, X. Xu, and B. Pfeiffer, *Chinese Physics C* **36**, 1287 (2012).
- [48] J. M. Pearson, S. Goriely, and N. Chamel, *Physical Review C* **83** (2011), 10.1103/PhysRevC.83.065810.
- [49] N. Chamel, E. Molter, A. Fantina, and D. P. Arteaga, *Physical Review D* **90** (2014), 10.1103/PhysRevD.90.043002.
- [50] G. Gamow, *Physical Review* **55**, 718 (1939).
- [51] S. Bonazzola, E. Gourgoulhon, M. Salgado, and J. Marck, *Astronomy and Astrophysics* **278**, 421 (1993).
- [52] M. Bocquet, S. Bonazzola, E. Gourgoulhon, and J. Novak, *Astron. Astrophys.* **301**, 757 (1995), arXiv:gr-qc/9503044 [gr-qc].
- [53] B. Franzon, V. Dexheimer, and S. Schramm, *Monthly Notices of the Royal Astronomical Society* **456**, 2937 (2016).
- [54] B. Franzon, V. Dexheimer, and S. Schramm, *Phys. Rev. D* **94**, 044018 (2016), arXiv:1606.04843 [astro-ph.HE].
- [55] B. Franzon, R. O. Gomes, and S. Schramm, *Mon. Not. Roy. Astron. Soc.* **463**, 571 (2016), arXiv:1608.02845 [astro-ph.HE].
- [56] E. Gourgoulhon, *3+1 formalism in general relativity: bases of numerical relativity*, Vol. 846 (Springer Science Business Media, 2012).
- [57] U. Das and B. Mukhopadhyay, *Physical Review Letters* **110**, 071102 (2013), arXiv:1301.5965 [astro-ph.SR].
- [58] C. Armaza, A. Reisenegger, and J. A. Valdivia, *The Astrophysical Journal* **802**, 121 (2015).
- [59] J. Mitchell, J. Braithwaite, A. Reisenegger, H. Spruit, J. Valdivia, and N. Langer, *Monthly Notices of the Royal Astronomical Society* **447**, 1213 (2015).
- [60] J. Braithwaite, *Astronomy & Astrophysics* **453**, 687 (2006).
- [61] P. Bera and D. Bhattacharya, (2016), arXiv:1607.06829 [astro-ph.SR].
- [62] P. Goldreich and A. Reisenegger, *The Astrophysical Journal* **395**, 250 (1992).